npj | Climate and Atmospheric Science

www.nature.com/npjclimatsci

ARTICLE OPEN

^{10}Be age constraints on latest Pleistocene and Holocene cirque glaciation across the western United States

Shaun A. Marcott[1], Peter U. Clark[2], Jeremy D. Shakun[3], Edward J. Brook[2], P. Thompson Davis[4] and Marc W. Caffee[5,6]

Well-dated records of alpine glacier fluctuations provide important insights into the temporal and spatial structure of climate variability. Cirque moraine records from the western United States have historically been interpreted as a resurgence of alpine glaciation in the middle-to-late Holocene (i.e., Neoglaciation), but these moraines remain poorly dated because of limited numerical age constraints at most locations. Here we present 130 ^{10}Be ages on 19 moraines deposited by 14 cirque glaciers across this region that have been interpreted as recording these Neoglacial advances. Our ^{10}Be chronology indicates instead that these moraines were deposited during the latest Pleistocene to earliest Holocene, with several as old as 14–15ka. Our results thus show that glaciers retreated from their Last Glacial Maximum (LGM) extent into cirques relatively early during the last deglaciation, experienced small fluctuations during the Bølling–Allerød–Younger Dryas interval, and remained within the maximum limit of the Little Ice Age (LIA) advance of the last several centuries throughout most of the Holocene. Climate modeling suggests that increasing local summer insolation and greenhouse gases were the primary controls on early glacier retreat from their LGM positions. We then infer that subsequent intrinsic climate variability and Younger Dryas cooling caused minor fluctuations during the latest Pleistocene, while the LIA advance represents the culmination of a cooling trend through the Holocene in response to decreasing boreal summer insolation.

npj Climate and Atmospheric Science (2019)2:5 ; https://doi.org/10.1038/s41612-019-0062-z

INTRODUCTION

Glaciers are among the most sensitive responders to climate change, and their well-documented retreat over the past century is a clear signal of global warming.[1–3] Long records of glacier fluctuations provide an important context for assessing the role of natural variability on this recent glacier retreat, helping to isolate an anthropogenic signal.[4] Research over the past century established the current paradigm that warmth during the early-to-middle Holocene caused widespread retreat of high-altitude cirque glaciers in the western United States, followed by a resurgence of alpine glaciation, or Neoglaciation,[5] beginning after 6ka (Fig. 2b), with the most recent advance during the Little Ice Age (LIA).[6,7] The ages of these cirque moraines, which exist just distal to the LIA moraines, were largely determined using relative dating techniques.[8–11] The moraines were then correlated with similar moraines that represented the type sites of Neoglacial events across the American West, such as Temple Lake in Wyoming,[12] TL in Colorado,[13] and Recess Peak in California.[14] The numerical ages of these type moraines, however, were also not well constrained, and in the few instances where numerical dating was subsequently applied,[15,16] some of these moraines have instead been attributed to the late-Pleistocene Younger Dryas cold event (12.9–11.7 ka).[17–20] The ages of nearly all of these particular cirque moraines thus remain highly uncertain,[21] which has important implications for our general understanding of Holocene climate,[22] glacier change,[23] proposed rapid climate change events during the Holocene,[24] and silicate weathering estimates.[25,26] Moreover, the presence of Neoglacial moraines beyond the LIA extent would imply a cooler pre-LIA climate, in contrast to regional and hemispheric temperature reconstructions[22] that show a cooling trend through the middle-to-late Holocene culminating with maximum cooling during the LIA.

Here we address these issues by using cosmogenic ^{10}Be to date 130 boulders from 19 moraines deposited by 14 cirque glaciers across the western United States (U.S.) (Fig. 1) that were previously interpreted as Neoglacial or early Holocene in age (Fig. 2) (see Supplementary Discussion). Our ^{10}Be chronology demonstrates that each of the moraines originally interpreted as Neoglacial was deposited during the latest Pleistocene to earliest Holocene (between ~15 and 9 ka), indicating that, with the exception of some isolated locations,[27,28] cirque glaciers in the western U.S. did not extend beyond their LIA limits during much, if not all, of the Holocene.

RESULTS

Moraine chronologies

Moraines sampled for ^{10}Be dating are 15–30 km up-valley from moraines marking the Last Glacial Maximum (LGM) and <2 km from cirque headwalls. The moraines in 10 cirques occur just distal (within several hundred meters) to presumed LIA moraines or associated rock glaciers, while no LIA-associated moraine or rock glacier occurs up-valley in the other four cirques. We interpret the ^{10}Be ages to represent the time of onset of glacier retreat from the

[1]Department of Geoscience, University of Wisconsin-Madison, Madison, WI 53706, USA; [2]College of Earth, Ocean, and Atmospheric Sciences, Oregon State University, Corvallis, OR 97331, USA; [3]Department of Earth and Environmental Sciences, Boston College, Chestnut Hill, MA 02467, USA; [4]Department of Natural and Applied Sciences, Bentley University, Waltham, MA 02452, USA; [5]Department of Physics and Astronomy, Purdue University, West Lafayette, IN 47907, USA and [6]Department of Earth, Atmospheric, and Planetary Sciences, Purdue University, West Lafayette, IN 47907, USA
Correspondence: Shaun A. Marcott (smarcott@wisc.edu)

Received: 19 September 2018 Accepted: 4 January 2019
Published online: 30 January 2019

Published in partnership with CECCR at King Abdulaziz University

npj nature partner journals

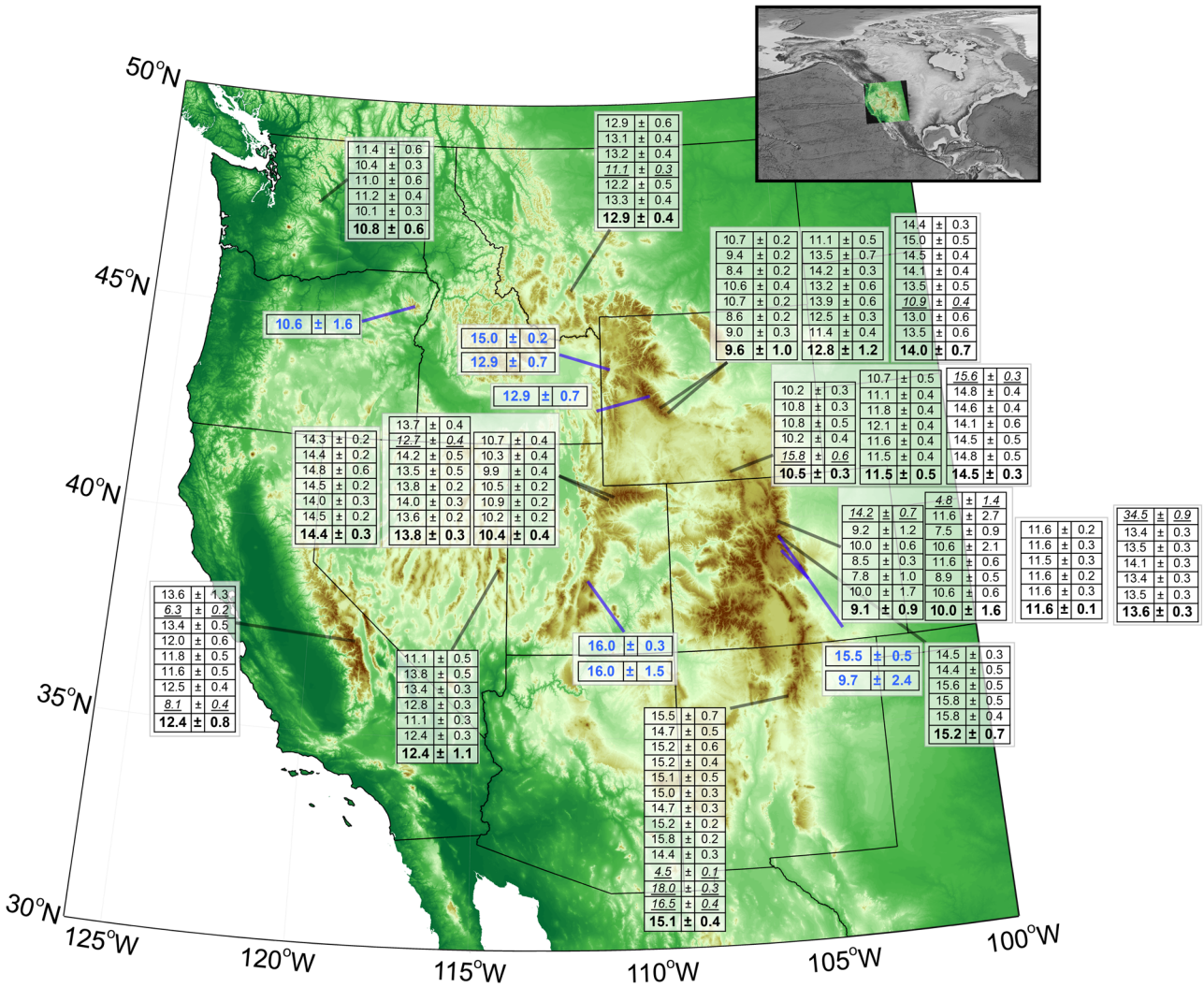

Fig. 1 Shaded relief map of the western United States, sample locations, and moraine boulder ages. Boxes indicate individual boulder ages and uncertainties (regular font) and the arithmetic mean moraine age and standard deviation (bold) from this study. Italicized and underlined ages are outliers as defined in the text. Moraine arithmetic mean ages and uncertainties (standard deviation) from prior surface exposure age dating studies are also provided (blue font)

moraines. The age of each moraine and its uncertainty is reported as the arithmetic mean and standard deviation (1σ) of the ^{10}Be ages, and we add the production rate uncertainty (~1–5%) in quadrature when comparing our ages to records based on other dating methods. See Methods section for details on sample preparation and age calculations.

Based on geomorphic relations and the precision of our ages, we can distinguish at least six discrete episodes of moraine-building events (Fig. 2b), with three latest Pleistocene cirque-glacier events occurring prior to the Younger Dryas cold interval, one within the interval, and two after. To constrain the event ages, we only consider analytical uncertainty in the ^{10}Be ages because of equivalent production rate uncertainty. Moraines representing the discrete events are identified by either being from stratigraphically distinct moraines from the same cirque or by differing in age at 1σ from the other events (Table S1). The moraines from the Medicine Bow Mountains (MB) in the Snowy Range of southeastern Wyoming alone identify three distinct events, with their ages confirming a millennial-scale signal (14.5 ± 0.3, 11.5 ± 0.3, and 10.5 ± 0.3 ka). The oldest moraine ages from the Lake Katherine (LK) moraine in the Sangre de Cristo Mountains, New Mexico (15.1 ± 0.4 ka), the Upper Chicago Lake (CL) moraine in the Colorado Front Range (15.2 ± 0.7 ka), and the Blue Lake (BL) moraine in the Uinta Mountains (14.4 ± 0.3 ka) overlap with the oldest moraine age from the Snowy Range (14.5 ± 0.3 ka) and may thus be part of the same event. The age of the Deadhorse (DH) moraine in the Uinta Mountains of Utah (13.8 ± 0.3 ka) falls between the ages of the two older moraines from the Snowy Range and records a second event. Multiple other sites record moraine ages from 13 to 12 ka that overlap with each other at 1σ (Fig. 2b), but only the Horse Mountain (HM) moraine in the Tobacco Root Mountains, Montana (12.9 ± 0.4 ka) demonstrates a distinct third event. The age of the Fourth of July (FJ) moraine in the Colorado Front Range (11.6 ± 0.1 ka) is included with the intermediate Snowy Range moraine (11.5 ± 0.3 ka) to record a fourth event. The youngest DH moraine in the Uinta Mountains (10.4 ± 0.4 ka) is included with the youngest Snowy Range moraine (10.5 ± 0.3 ka) as a fifth event. Finally, the youngest distinct event is recorded by the inner Triple Lakes (TL) moraine from the Colorado Front Range (9.1 ± 0.9 ka).

Glacier length changes

In order to quantify changes in glacier length relative to their LGM positions, we scaled glacier positions as marked by moraines from each valley to normalized unit lengths, from 1 at their LGM

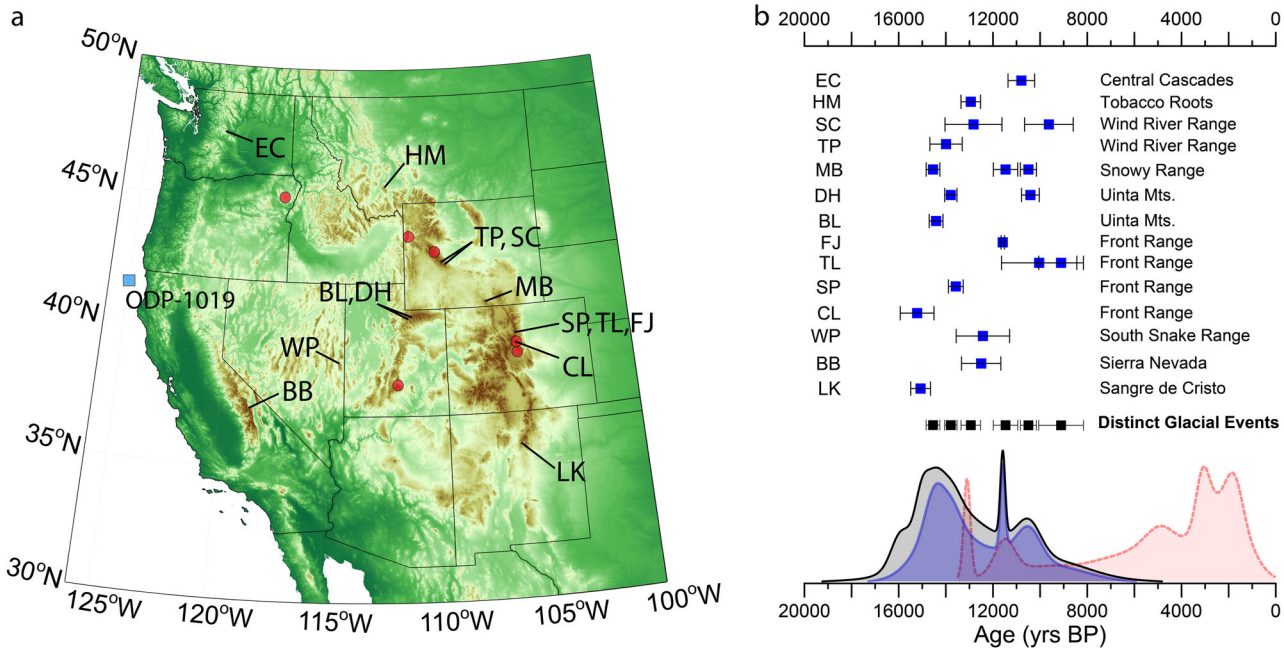

Fig. 2 Shaded relief map of the western United States with locations of records discussed, and moraines ages from this study. **a** Black lines with labels denote field locations for this study, red circles show six other locations where previous cosmogenic-based cirque moraine chronologies exist and have been recalibrated, [19,31,58–60] and blue box denotes location of a sea surface temperature record.[61] From south to north, LK—Lake Katherine; BB—Baboon Lakes; WP—Wheeler Peak; CL—Chicago Lakes; SP—Satanta Peak; TL—Triple Lakes; FJ—Fourth of July; BL—Blue Lake; DH—Deadhorse Lake; MB—Medicine Bows; TP—Temple Peak; SC—Stough Creek; HM—Horse Mountain; EC—Enchantment Lakes Basin. **b** Arithmetic mean (blue squares) and standard deviation (1σ) of boulder ages from moraine crests and distinct glacial events (black squares) based on moraine ages and stratigraphic positions from this study (see text). The lower curves show a probability density function of all ^{10}Be ages from this study (blue curve and fill) and combined with recalibrated ages from six other locations (black curve and fill), and an approximate density curve based on previously interpreted ages of moraines from this study (pink dotted curve and fill)

positions to 0 at cirque headwalls (Fig. 1f). Although not necessarily a simple function of climate, previous work[1,29,30] demonstrates that records of change in glacier length over large geographic areas capture first-order patterns of glacier response to climate. We combined our data with cosmogenic exposure ages from other moraines in the western U.S., with all ages recalibrated to be consistent with our ages (Figs. 1 and 2).

This compilation shows that most glaciers began retreating from their LGM moraines between 22 and 18 ka (ref. [30]). The LK moraine from the Sangre de Cristo Mountains, New Mexico, together with moraines of similar age from the Colorado Front Range, Snowy Range, and the Yellowstone region of Wyoming, reveal 75–90% of retreat from LGM limits by ~15 ka, when simulations with a global climate model suggest that deglacial warming for this region had only reached ~50% of interglacial values (Fig. 3f). Such a nonlinear response may be due to hypsometric factors[30] or, in the case of the Yellowstone Ice Cap, dynamic controls.[31] By 14–13 ka, glaciers across most of the western U.S. had retreated by at least 90% to reach new high-elevation positions and deposit moraines 1–2 km from cirque headwalls (Fig. 3f). We attribute this regional-scale glacier recession primarily to warming, since its spatial coherency and magnitude are unlikely to be explained by changes in precipitation.[32] Transient climate modeling shows that the combination of increasing boreal summer insolation[33] (Fig. 3a) and atmospheric CO_2 (ref. [34]) (Fig. 3b) caused the warming that led to this widespread deglaciation of western U.S. glaciers (Fig. 3f).

DISCUSSION

Glacial events from ~15 to 13 ka occurred when simulated interglacial summer temperatures in the western U.S. were largely established (Fig. 3f) and atmospheric carbon dioxide levels were relatively stable (Fig. 3b). Such glacier variability may thus reflect forcing by natural modes of multidecadal climate variability that influences the western U.S. glaciers.[35] Alternatively, modeling has shown that even in a stable climate, stochastic interannual variability can lead to kilometer-scale changes in glacier length on centennial to millennial timescales.[36,37] Our data also identify cirque-glacier fluctuations that fall within the Younger Dryas cold interval (Fig. 2b), suggesting a forced response to this event that has been identified in other western U.S. paleoclimate proxy records.[38–41]

Of the 19 moraines dated in this study, six have mean ages that indicate glaciers in some parts of the western U.S. persisted until the early Holocene (Fig. 2b). Model simulations indicate that maximum Holocene summer temperatures occurred between 11 and 9 ka in response to summer insolation (Fig. 3f), which is generally consistent with sea surface temperatures off the Oregon and Alaskan coasts (Fig. 3d, e), while our data suggest that some glaciers persisted during this warmest interval. Similar to the latest Pleistocene moraines, glacier variability during the earliest Holocene suggested by the moraine ages may have been forced by centennial to decadal climate variability and/or stochastic interannual climate variability. Following this final glacier phase, remaining cirque glaciers retreated further and may have completely disappeared in the western U.S. before onset of Neoglaciation some 7–6kyr later that led to renewed glacier growth, culminating in the LIA.[17,21,23,42] We thus conclude that the LIA-associated moraines in western North America represent the most extensive glaciation of the last ~11–10ka, likely in response to a decrease in boreal summer insolation[33] (Fig. 3a) and regional (Fig. 3f) and hemispheric (Fig. 3b) cooling through the mid-to-late

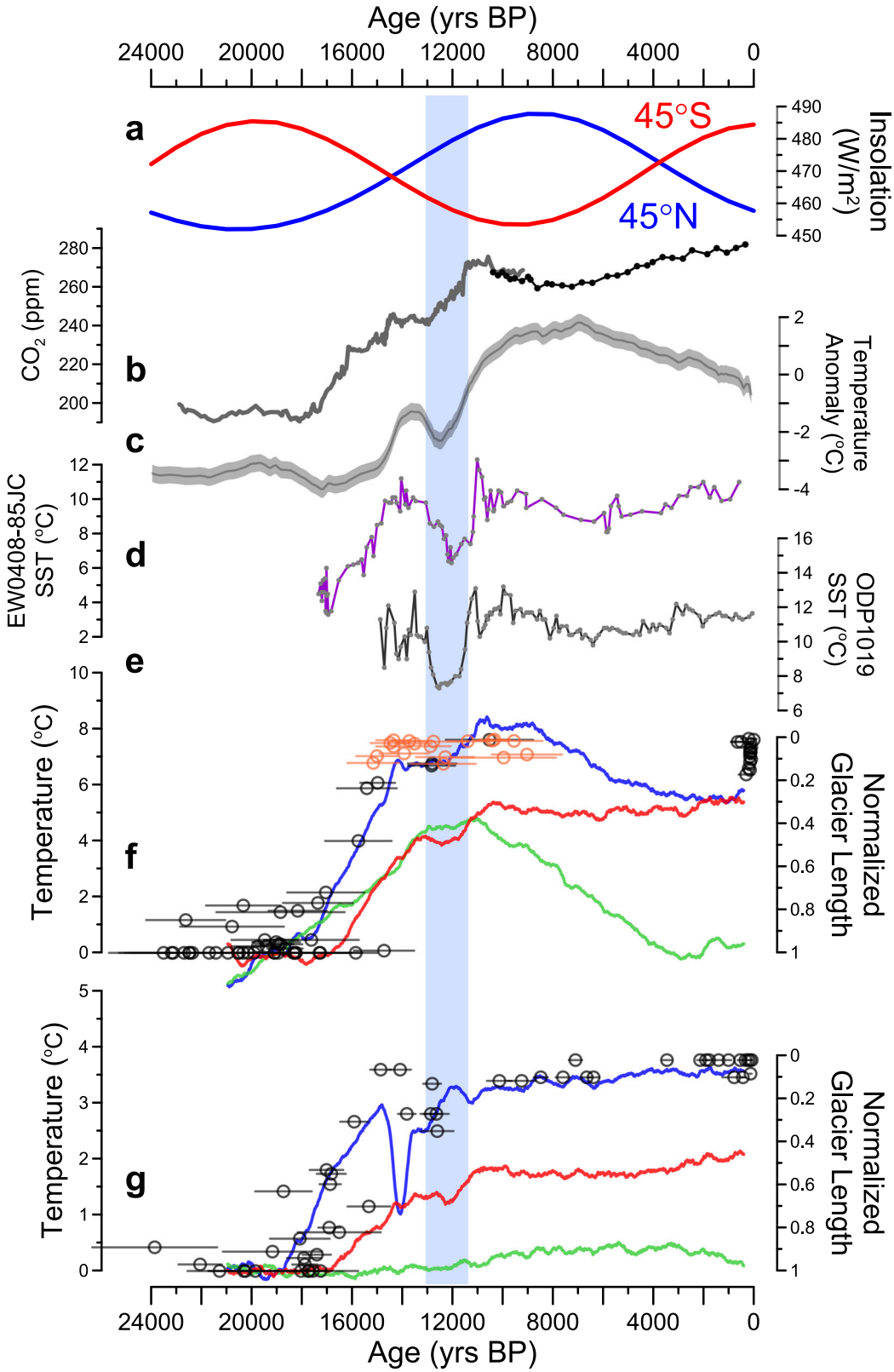

Holocene,[22] resulting in any record of earlier Neoglaciation being overridden by the LIA advance.

The glacial records from the western U.S. are in good agreement with well-dated records from the European Alps, which show that after retreating from their LGM positions to high-elevation cirques by ~15–13 ka, glaciers remained within their LIA limits throughout the Holocene.[43,44] Glaciers in the Southern Alps of New Zealand also retreated far up-valley from their LGM positions by 15ka (Fig. 3g),[45,46] consistent with a dominant greenhouse gas forcing that synchronized deglaciation in the two

Fig. 3 Normalized moraine distance from cirque headwalls through the last deglaciation across the western United States compared to reconstructed and simulated climate forcing. **a** Summer insolation at 45°N (JJA) and 45°S (DJF) (ref. [62]). **b** Atmospheric carbon dioxide concentrations from the WDC and EPICA ice cores.[34,63,64] **c** Northern hemisphere multiproxy temperature reconstruction for 30–60°N (refs. [22,48]). **d**, **e** Sea surface temperatures off the northern California (ODP1019)[61] and southern Alaskan (EW0408-85JC)[38] coasts. **f**, **g** Normalized distances between LGM moraines and cirque headwalls in the western U.S. (**f**—this study and calculated results from ref. [30]) and from New Zealand and Australia (**g**—calculated results from ref. [30]), and simulated local summer temperatures from transient modeling.[47,65] Orange (this study) and black (from ref. [30]) circles are the mean of boulder surface exposure ages on each moraine and the bars represent the standard deviation (1σ) of the boulder ages and the production rate uncertainty, added in quadrature. The simulated temperatures are for the ALL (blue) and single-forcing orbital (green) and greenhouse gas (red) simulations. The blue vertical bar represents the YD interval, the end of which corresponds to the Pleistocene/Holocene boundary. EPICA European Project for *Ice* Coring in Antarctica, WDC West Antarctic Ice Sheet Divide ice core, LGM Last Glacial Maximum, YD Younger Dryas cold period

hemispheres.[30] In contrast to the western U.S. and European Alps, however, glaciers in the Southern Alps of New Zealand then re-advanced during the Antarctic Cold Reversal,[45] retreated during the Younger Dryas,[46] and then continued to slowly retreat throughout the Holocene to their LIA positions[45] (Fig. 3g). Transient climate modeling suggests that this anti-phased hemispheric glacier behavior during the Holocene (Northern Hemisphere regrowth and advance, Southern Hemisphere retreat) occurred in response to differing combinations of orbital and greenhouse gas forcing.[30] In the Northern Hemisphere, the large decrease in summer insolation following its peak at ~8 ka dominated the temperature response, leading to cooling throughout the Holocene (Fig. 3f). In contrast, Southern Hemisphere glaciers experienced rising local summer insolation throughout the Holocene, leading to relatively cooler early Holocene temperatures that subsequently warmed (Fig. 3g). Thus, while glacial retreat in the two hemispheres was largely in phase during the last deglaciation, the hemispheric response became out of phase during the Holocene (Fig. 3f, g). This change in glacier response was likely caused by a switch from greenhouse gas-dominated forcing from ~18 to 11 ka during the last deglaciation[47,48] to largely local summer insolation forcing through the Holocene. The general advance of glaciers during the LIA in both the Northern and Southern hemispheres remains an enigma, but may be related to complex global climate feedbacks driven by solar minima and more frequent explosive volcanism.[49,50] The global retreat of alpine glaciers over the past century, however, indicates that the system has switched again to one dominated by greenhouse gas forcing,[4] but now associated with anthropogenic carbon emissions.

METHODS

Sample collection

Samples for surface exposure dating were collected from the tops of boulders resting on moraine crests at all of the field sites (Fig. S1) using hammers and chisels. Special care was taken to select boulders that met the following criteria: ~0.5 m or taller to limit the potential for excessive snow cover, or prior burial; resting on moraine crests to minimize chances of overturning or toppling during moraine degradation; little-to-no surface weathering features (e.g., pitting, exfoliation); and flat tops and/or simple surface geometries to limit uncertainties made for shielding calculations. Approximately 1–3 kg samples were collected from the top 2–4 cm of each boulder for cosmogenic nuclide chemistry and analyses. Shielding measurements were made in the field using a Suunto clinometer and boulder surface geometries were measured using a Brunton compass. Latitude, longitude, and elevation for each boulder were collected using a handheld Global Positioning System and crosschecked with topographic maps.

Laboratory Techniques

We prepared samples for ^{10}Be analysis at Oregon State University and the University of Wisconsin-Madison following the methods of Licciardi[51] and Rinterknecht,[52] with modifications by Goehring.[53] The top 1–2 cm of each sample was crushed in a Bico disk mill and sieved to the 250–710 µm size fraction. The magnetic fraction of each sample was removed using a Frantz Isodynamic Mineral Separator. All samples were first leached for 24–48 h in 5–10% HNO_3 and then for an additional 24–72 h in a 1% HNO_3 + 1% hydrogen fluoride (HF) solution in warm ultrasonic baths to remove all non-quartz minerals and meteoric ^{10}Be from the quartz surfaces. Small subsamples were then analyzed for Al, Ca, Fe, K, Mg, Na, and Ti by inductively coupled plasma-optical spectroscopy following digestion in HF to determine quartz purity; samples were leached further if purity criteria were not met. After sufficient purity was obtained, 20–50 g of sample together with ~0.25–0.75 µg of Be carrier were added to Teflon beakers and dissolved in concentrated HF. The HF was then evaporated and several $HClO_4$ and HCl evaporations were performed to convert the samples to chloride form. Samples were then passed through cation and anion exchange columns to isolate Be. After completing the chromatography, the pH of each sample was adjusted to 5 with NH_4OH to precipitate any Ti remaining in the sample as $Ti(OH)_4$, which was removed by centrifugation. Following the Ti-removal, the pH of each sample was adjusted to 8 to precipitate $Be(OH)_2$ and then washed three times in ultrapure water adjusted to pH 8 to remove boron. The samples were transferred to acid-cleaned, low-Boron quartz crucibles and evaporated at 80–90 °C in a high efficiency particulate air filter laminar flow bench. The $Be(OH)_2$ was then converted to BeO by heating the covered crucibles in a rapid mineralizer for 60 min at 999 °C. Finally, samples were packed into targets in a laminar flow hood for accelerator mass spectrometry (AMS) analysis at the Purdue Rare Isotope Measurement (PRIME) Laboratory.

Each batch of samples was processed with one or two system blanks to account for background ^{10}Be introduced during processing or AMS measurement. Additionally, we made repeated measurements ($n = 7$) from a single sample (DPI-MB-01) throughout the duration of the project, as well as a limited number of replicate measurements ($n = 3$) for another sample (LL-MB-07). The standard error of the replicate measurements for DPI-MB-01 (350 yr) is equal to the internal uncertainty of the sample (see Supplementary Data file).

Exposure age calculations

After correcting for the system blank (<1%), ^{10}Be concentrations in quartz were calculated from the ^{10}Be/^{9}Be ratio and carrier and sample amounts. Exposure ages were calculated for each boulder following the methods and online program of the CRONUS Online Calculator v.3 (ref. [54]). All raw ^{10}Be/^{9}Be measurements were calibrated against the Revised ICN Standard (07KNSTD) following the protocol outlined by PRIME Lab. Cosmogenic nuclide exposure ages were calculated using the scaling model LSDn and the regional production rate of 3.92 ± 0.31 atom g^{-1} yr^{1} from Promontory Point in Utah.[55]

To calculate moraine ages and their uncertainties, we report the arithmetic mean of the boulder exposure ages and the standard deviation (1σ), but include alternate mean-age and uncertainty calculations in the Supplementary Data file. Outliers in a set of boulder ages from a single moraine are initially defined as being >5 standard deviations from the mean value of the other boulder exposure ages following a similar method as Putnam et al.[56] This method of identifying outliers accounts for 4 of the 14 identified in this dataset. We then used Chauvenet's criterion to identify ten additional outliers (see Supplementary Data file).

Because the majority of the boulders sampled had pristine surfaces that showed no clear post-depositional weathering features and were generally glacially polished and/or striated, we do not apply an erosion correction to our surface exposure ages. We also do not apply a snow correction to our surface exposure ages, as no correlation between boulder height and surface exposure age is distinguishable from our dataset, and we consider our boulder sampling sites, which are from the exposed moraine ridges, to be generally wind swept throughout the year. However, assuming our

boulder ages were covered by 0.5 m of snow ($\rho = 0.3$ g cm^{-3}) for 4 months of the year, a correction of ~3% would be necessary,[57] which is well within the age uncertainties from the scaling and production calculations.

DATA AVAILABILITY

All data generated or analyzed during this study are included in this published article as a Supplemental Data file.

ACKNOWLEDGEMENTS

We thank P. Birkeland, G. Bucci, J. Clague, J. Clark, D. Dahms, S. Davis, V. Ersek, B. Goehring, B. Menounos, A. Novak, G. Osborn, and M. Ravesi for field work assistance; G. Baker, H. Basagic, A. Fountain, S. Hostetler, B. Laabs, J. Licciardi, G. Osborn, and G. Stock for discussions; S. Ma and T. Woodruff at PRIME Lab for assistance in AMS sample preparation; A. Barth, L. Farmer, C. Carlson-Ham, A. Novak, C. Vavrus, and K. Zahnle-Hostetler for lab assistance; and the U.S. National Park Service and U.S. Forest Service for permission to access field sites. This work was supported by National Science Foundation grants EAR 0746375 (P.U.C., E.J.B., and P.T.D.), BCS 0802842 (P.U.C. and S.A.M.), and EAR 1153689 (M.W.C.), a Bentley University faculty grant (P.T.D.), a Geological Society of America research grant (S.A.M.), and scholarships to SAM from Oregon State University.

AUTHOR CONTRIBUTIONS

S.A.M and P.U.C. conceived the project and led the writing of the manuscript. S.A.M. led the field work and laboratory analyses. P.T.D. and J.D.S. assisted with field work, and E.J.B. assisted with laboratory analyses. M.W.C. oversaw the AMS procedures and measurements. All authors contributed to the writing of the manuscript.

ADDITIONAL INFORMATION

Supplementary information accompanies the paper on the *npj Climate and Atmospheric Science* website (https://doi.org/10.1038/s41612-019-0062-z).

Competing interests: The authors declare no competing interests.

Publisher's note: Springer Nature remains neutral with regard to jurisdictional claims in published maps and institutional affiliations.

REFERENCES

1. Oerlemans, J. Extracting a climate signal from 169 glacier records. *Science* **308**, 675–677 (2005).
2. Roe, G. H., Baker, M. B. & Herla, F. Centennial glacier retreat as categorical evidence of regional climate change. *Nat. Geosci.* **10**, 95–99 (2017).
3. Vaughan, D. G. et al. in *Climate Change 2013: The Physical Science Basis. Contribution of Working Group I to the Fifth Assessment Report of the Intergovernmental Panel on Climate Change* (eds Stocker, T.F., Qin D., Plattner G.-K., Tignor M., Allen S.K., Boschung J., Nauels A., Xia Y., Bex V. and Midgley P.M.) (Cambridge University Press, Cambridge, 2013).
4. Marzeion B., Cogley J. G. Richter K. & Parkes D. Attribution of global glacier mass loss to anthropogenic and natural causes. *Science* **345**, 919–921 (2014).
5. Porter, S. C. & Denton, G. H. Chronology of Neoglaciation in the North American Cordillera. *Am. J. Sci.* **265**, 177–210 (1967).
6. Matthes, F. E. Multiple glaciations in the Sierra Nevada. *Science* **70**, 75–76 (1929).
7. Salisbury R. D., & Blackwelder E. Glaciation in the Bighorn Mountains. *J. Geol.* **11**, 216–223 (1903).
8. Burke, R. M. & Birkeland, P. W. Reevaluation of multiparameter relative dating techniques and their application to the glacial sequence along the eastern escarpment of the Sierra Nevada, California. *Quat. Res.* **11**, 21–51 (1979).
9. Burke, R. M. *Multiparameter Relative Dating (RD) Techniques Applied to Morainal Sequences Along the Eastern Sierra Nevada, California and Wallowa Lake Area, Oregon* (University of Colorado-Boulder, Colorado, 1979).
10. Vreeken, W. J. in *Quaternary Dating Methods* 269–281 (Elsevier Science Publishers, 1984).
11. Burke, R. M. & Birkeland, P. W. in Wright, H. E. ed. *Late Quaternary Environments of the United States* (ed. Mahaney, W. C.) 3–11 (University of Minnesota Press, Minneapolis, 1983).
12. Richmond, G. M. in *The Quaternary of the United States* (eds Wright Jr., H. E. & Frey, D. G.) 217–230 (Princeton University Press, Princeton, 1965).
13. Benedict, J. B. Chronology of cirque glaciation, Colorado Front Range. *Quat. Res.* **3**, 584–599 (1973).
14. Birman, J. H. Glacial Geology across the Crest of the Sierra Nevada, California. *Calif. Geol Soc. Am. Spec. Paper* **75**, 80 (1964).
15. Zielinski, G. A. & Davis, P. T. Late Pleistocene age of the type Temple Lake moraine, Wind River Range, Wyomong, USA. *Geogr. Phys. Quat.* **41**, 397–401 (1987).
16. Clark, D. H. & Gillespie, A. R. Timing and significance of late-glacial and Holocene cirque glaciation in the Sierra Nevada, California. *Quat. Int.* **38/39**, 21–38 (1997).
17. Davis, P. T., Menounos, B. & Osborn, G. Holocene and latest Pleistocene alpine glacier fluctuations: a global perspective. *Quat. Sci. Rev.* **28**, 2021–2033 (2009).
18. Davis, P. T. & Osborn, G. Age of pre-Neoglacial cirque moraines in the central in the Central North American Cordillera. *Géogr. Phys. Quat.* **41**, 365 (1987).
19. Gosse, J. C., Evenson, E. B., Klein, J., Lawn, B. & Middleton, R. Precise cosmogenic ^{10}Be measurements in western North America: support for a global Younger Dryas cooling event. *Geology* **23**, 877–880 (1995).
20. Menounos, B. & Reasoner, M. A. Evidence for cirque glaciation in the Colorado Front Range during the Younger Dryas chronozone. *Quat. Res.* **48**, 38–47 (1997).
21. Davis, P. T. Holocene glacier fluctuations in the American Cordillera. *Quat. Sci. Rev.* **7**, 129–157 (1988).
22. Marcott, S. A., Shakun, J. D., Clark, P. U. & Mix, A. C. A reconstruction of regional and global temperature for the past 11,300 years. *Science* **339**, 1198–1201 (2013).
23. Solomina, O. N. et al. Holocene glacier fluctuations. *Quat. Sci. Rev.* **111**, 9–34 (2015).
24. Mayewski, P. A. et al. Holocene climate variability. *Quat. Res.* **62**, 243–255 (2004).
25. Blum, J. D. & Erel, Y. A silicate weathering mechanism linking increases in marine ^{87}Sr/^{86}Sr with global glaciation. *Nature* **373**, 415–418 (1995).
26. Taylor, A. & Blum, J. D. Relation between soil age and silicate weathering rates determined from the chemical evolution of a glacial chronosequence. *Geology* **23**, 979–982 (1995).
27. Marcott, S. A., Fountain, A., O'Connor, J. E., Sniffen, P. J. & Dethier, D. P. A latest Pleistocene and Holocene glacial history and paleoclimate reconstruction at Three Sisters and Broken Top Volcanoes, Oregon, U.S.A. *Quat. Res.* **71**, 181–189 (2009).
28. Menounos, B. et al. Did rock avalanche deposits modulate the late Holocene advance of Tiedemann Glacier, southern Coast Mountains, British Columbia, Canada? *Earth Planet. Sci. Lett.* **384**, 154–164 (2013).
29. Young, N. E., Briner, J. P., Leonard, E. M., Licciardi, J. M. & Lee, K. Assessing climatic and nonclimatic forcing of Pinedale glaciation and deglaciation in the western United States. *Geology* **39**, 171–174 (2011).
30. Shakun, J. D. et al. Regional and global forcing of glacier retreat during the last deglaciation. *Nat. Commun.* **6**, 8059 (2015).
31. Licciardi, J. M. & Pierce, K. L. Cosmogenic exposure-age chronologies of Pinedale and Bull Lake glaciations in greater Yellowstone and the Teton Range, U.S.A. *Quat. Sci. Rev.* **27**, 814–831 (2008).
32. Hostetler, S. W. & Clark, P. U. Climatic controls of western US glaciers at the last glacial maximum. *Quat. Sci. Rev.* **16**, 505–511 (1997).
33. Berger, A. & Loutre, M.-F. Insolation values for the climate of the last 10 million years. *Quat. Sci. Rev.* **10**, 297–317 (1991).
34. Marcott, S. A. et al. Centennial-scale changes in the global carbon cycle during the last deglaciation. *Nature* **514**, 616–619 (2014).
35. Bitz, C. M. & Battisti, D. S. Interannual to decadal variability in climate and the glacier mass balance in Washington, western Canada, and Alaska. *J. Clim.* **12**, 3181–3196 (1999).
36. Roe, G. H. & O'Neal, M. A. The response of glaciers to intrinsic climate variability: observations and models of late-Holocene variations in the Pacific Northwest. *J. Glaciol.* **55**, 839–854 (2009).
37. Barth, A. M. et al. Persistent millennial-scale glacier fluctuations in Ireland between 24 ka and 10 ka. *Geology* **46**, 151–154 (2018).
38. Praetorius, S. K. et al. North Pacific deglacial hypoxic events linked to abrupt ocean warming. *Nature* **527**, 362–366 (2015).
39. Vacco, D. A., Clark, P. U., Mix, A. C., Cheng, H. & Edwards, R. L. A speleothem record of Younger Dryas cooling, Klamath Mountains, Oregon, USA. *Quat. Res.* **64**, 249–256 (2005).
40. Mix, A. C. et al. Rapid climate oscillations in the northeast Pacific during the last deglaciation reflect Northern and Southern Hemisphere sources. In: *Mechanisms of Global Climate Change at Millennial Time Scales*, AGU Monograph. (eds. Clark, P. U., Webb, R.S., Keigwin, L.D.) (American Geophysical Union, Washington, DC, 127–148, 1999).
41. MacDonald, G. M. et al. Evidence of temperature depression and hydrological variations in the eastern Sierra Nevada during the Younger Dryas stade. *Quat. Res.* **70**, 131–140 (2008).
42. Solomina, O. N. et al. Glacier fluctuations during the past 2000 years. *Quat. Sci. Rev.* **149**, 61–90 (2016).
43. Ivy-Ochs, S. et al. The timing of glacier advances in the northern European Alps based on surface exposure dating with cosmogenic ^{10}Be, ^{26}Al, ^{36}Cl, and ^{21}Ne. *Geol. Soc. Am. Spec. Paper* **415**, 43–60 (2006).
44. Ivy-Ochs, S. et al. Latest Pleistocene and Holocene glacier variations in the European Alps. *Quat. Sci. Rev.* **28**, 2137–2149 (2009).

45. Putnam, A. E. et al. Regional climate control of glaciers in New Zealand and Europe during the pre-industrial Holocene. *Nat. Geosci.* **5**, 627–630 (2012).
46. Kaplan, M. R. et al. Glacier retreat in New Zealand during the Younger Dryas stadial. *Nature* **467**, 194–197 (2010).
47. Liu, Z. et al. Transient simulation of last deglaciation with a new mechanism for Bølling–Allerød warming. *Science* **325**, 310–314 (2009).
48. Shakun, J. D. et al. Global warming preceded by increasing carbon dioxide concentrations during the last deglaciation. *Nature* **484**, 49–54 (2012).
49. Miller, G. H. et al. Abrupt onset of the Little Ice Age triggered by volcanism and sustained by sea-ice/ocean feedbacks. *Geophys. Res. Lett*. **39**, (2012).
50. Orsi, A. J., Cornuelle, B. D. & Severinghaus, J. P. Little Ice Age cold interval in West Antarctica: Evidence from borehole temperature at the West Antarctic Ice Sheet (WAIS) Divide: WAIS DIVIDE TEMPERATURE. Geophys. Res. Lett. 39, (2012).
51. Licciardi, J. F. *Alpine Glacier and Pluvial Lake Records of Late Pleistocene Climate Variability in the Western United States* (Oregon State University, Department of Geosciences, Oregon, 2000).
52. Rinterknecht, V. R. *Cosmogenic 10-Be Chronology for the Last Deglaciation of the Southern Scandinavian Ice Sheet* (Oregon State University, Department of Geosciences, Oregon, 2004).
53. Goehring, B. M. *^{10}Be Exposure Ages of Erratic Boulders in Southern Norway and Implications for the History of the Fennoscandian Ice Sheet* (Oregon State University, Department of Geosciences, Oregon, 2006).
54. Marrero, S. M. et al. Cosmogenic nuclide systematics and the CRONUScalc program. *Quat. Geochronol.* **31**, 160–187 (2016).
55. Lifton, N. A *et al.* A new estimate of the spallogenic production rate of in situ cosmogenic 10Be from Lake Bonneville shoreline features, Promontory Point, Utah. *Quat. Geochonol*. **26**, 56-69 (2015).
56. Putnam, A. E. et al. Glacier advance in southern middle-latitudes during the Antarctic Cold Reversal. *Nat. Geosci.* **3**, 700–704 (2010).
57. Gosse, J. C. & Phillips, F. M. Terrestrial in situ cosmogenic nuclides: theory and application. *Quat. Sci. Rev.* **20**, 1475–1560 (2001).
58. Licciardi, J. M., Clark, P. U., Brook, E. J., Elmore, D. & Sharma, P. Variable responses of western US glaciers during the last deglaciation. *Geology* **32**, 81–84 (2004).
59. Benson, L., Madole, R. F., Kubik, P. & McDonald, R. Surface-exposure ages of Front Range moraines that may have formed during the Younger Dryas, 8.2 cal ka, and Little Ice Age events. *Quat. Sci. Rev.* **26**, 1638–1649 (2007).
60. Marchetti, D. W., Cerling, T. E. & Lips, E. W. A glacial chronology for the Fish Creek drainage of Boulder Mountain, Utah, USA. *Quat. Res.* **64**, 263–271 (2005).
61. Barron, J. A., Heusser, L., Herbert, T. D. & Lyle, M. High-resolution climatic evolution of coastal northern California during the past 16,000 years. *Paleoceanography* **18**, 1020 (2003).
62. Laskar, J. et al. A long term numerical solution for the insolation quantities of the Earth. *Astron. Astrophys.* **428**, 261–285 (2004).
63. Monnin, E. et al. Atmospheric CO_2 concentrations over the last glacial termination. *Science* **291**, 112–114 (2001).
64. Lourantou, A., Chappellaz, J., Barnola, J. M., Masson-Delmotte, V. & Raynaud, D. Changes in atmospheric CO_2 and its carbon isotopic ratio during the penultimate deglaciation. *Quat. Sci. Rev.* **29**, 1983–1992 (2010).
65. He, F. et al. Northern Hemisphere forcing of Southern Hemisphere climate during the last deglaciation. *Nature* **494**, 81–85 (2013).

Open Access This article is licensed under a Creative Commons Attribution 4.0 International License, which permits use, sharing, adaptation, distribution and reproduction in any medium or format, as long as you give appropriate credit to the original author(s) and the source, provide a link to the Creative Commons license, and indicate if changes were made. The images or other third party material in this article are included in the article's Creative Commons license, unless indicated otherwise in a credit line to the material. If material is not included in the article's Creative Commons license and your intended use is not permitted by statutory regulation or exceeds the permitted use, you will need to obtain permission directly from the copyright holder. To view a copy of this license, visit http://creativecommons.org/licenses/by/4.0/.

© The Author(s) 2019